View metadata, citation and similar papers at core.ac.uk

brought to you by CORE

provided by Elsevier - Publisher Connector

Progress in Natural Science: Materials International 26 (2016) 341–346

HOSTED BY

ELSEVIER

Contents lists available at ScienceDirect

Progress in Natural Science: Materials International

journal homepage: www.elsevier.com/locate/pnsmi

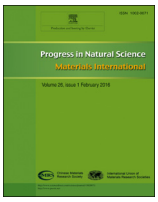

Original Research

Electrical conductivity retention and electrochemical activity of CSA doped graphene/gold nanoparticle@ polyaniline composites

Md. Akherul Islam [a], M. Ehtisham Khan [b], Muhammad Mohsin Hossain [b], Mudassir Hasan [b,*]

[a] Department of Pharmacy, Atish Dipankar University of Science & Technology, Banani, Dhaka 1213, Bangladesh
[b] School of Chemical Engineering, Yeungnam University, Gyeongsan 712-749, Republic of Korea

ARTICLE INFO

Article history:
Received 5 November 2015
Received in revised form
18 May 2016
Accepted 13 June 2016
Available online 18 June 2016

Keywords:
GN
GNP
Poly aniline
Conductivity retention
Thermal stability
Capacitor

ABSTRACT

This paper reports the synthesis of CTAB mediated CSA doped PANI and GN/GNP@ PANI composite nanofibers. The as synthesized composite nanofibers were examined by TEM, SEM, XRD, Raman spectroscopy; UV–visible diffused reflectance spectroscopy and TGA. The CTAB mediated CSA doped composite nanofibers showed 59% higher DC electrical conductivity at ambient temperature than that of PANI, which might be due to the enhancement in the mobility of the charge carriers and reduction in hopping distance in the composite system. The CTAB mediated CSA doped composite nanofibers compared to PANI was observed to be showing enhanced DC electrical conductivity retention after various cycles of heating, suggesting an enhancement in thermal stability of the composite structure, which could be attributed to the synergistic effect of GN, GNP and PANI. Additionally, the composite nanofibers showed greater electrochemical activity and better capacitive performance and reduced optical bandgap than that of PANI.

© 2016 Chinese Materials Research Society. Production and hosting by Elsevier B.V. This is an open access article under the CC BY-NC-ND license (http://creativecommons.org/licenses/by-nc-nd/4.0/).

1. Introduction

Amongst various conducting polymers, polyaniline (PANI) has attracted the attention of researchers globally owing to its low cost, ease of synthesis, remarkable electrochemical activity, and excellent doping de-doping chemistry [1–4]. Interestingly, nanostructured conducting polymers are suitable for various applications such as super-capacitors, batteries, chemical sensors and catalysis. Amongst the several nanostructures, PANI nanofibers have been studied widely owing to its high surface area and large ratio of length to diameter.

Graphene (GN) also has been studied extensively because of its high aspect ratio, excellent and unique thermal, mechanical and electrical properties [5,6]. Therefore, GN has opened several interesting and practical opportunity for it to be utilized in many applications, such as transparent electrodes, photovoltaic devices, super capacitors and chemical sensors [7–10].

Gold nanoparticles (GNP) owing to its unique catalytic and optical properties have been interesting and promising material [11]. The practical problem associated with the composite of polymer-metal nanoparticles arises due to metal nanoparticle's even dispersion into the entirety of PANI matrix. Due to this reason, an intimate contact between the metal nanoparticles and PANI matrix cannot be established resulting into weak interaction between PANI and metal nanoparticles. Another reason for weak interaction can be thought of as PANI and metal nanoparticles being heterogeneous might not intermix well. In the absence of intimate contact between metal particles and the polymer the physico-chemical properties remains unimproved.

In the past, several researchers reported the synthesis and physico-chemical characterization especially, electrical, electrochemical and sensing behavior of PANI/Graphite, PANI/Graphene oxide (GO), PANI/GO/GNP using different fabrication approaches [12–15].

To the best of the authors' knowledge, there are few reports on the synthesis and its detail physico-chemical properties of CSA doped graphene/gold nanoparticle@ PANI prepared under CTAB as surfactant. Therefore, more research is needed to establish the efficacy of gold nanoparticles into the PANI/GN composite system. This paper reports the fabrication of PANI and GN/GNP@ PANI composite nanofibers using a facile in-situ oxidative chemical polymerization technique. The thermal stability under DC electrical conductivity retention, electrochemical properties and optical properties has been studied in detail. The surface morphology, thermal, and micro structural properties were also investigated.

* Corresponding author.
E-mail address: hasanmudassir51@gmail.com (M. Hasan).
Peer review under responsibility of Chinese Materials Research Society.

http://dx.doi.org/10.1016/j.pnsc.2016.06.001
1002-0071/© 2016 Chinese Materials Research Society. Production and hosting by Elsevier B.V. This is an open access article under the CC BY-NC-ND license (http://creativecommons.org/licenses/by-nc-nd/4.0/).

2. Experimental

2.1. Materials

Aniline, gold nanoparticles (mean diameter ~10 nm) and camphorsulfonic acid (CSA) was purchased from Sigma Aldrich. Ammonium persulfate (APS), cetyltrimethylammonium bromide (CTAB), HCl, and methanol were supplied by Duksan pure chemicals, Korea, and used in synthesis as received. The water used in all the experiments was de-ionized water from a PURE ROUP 30 water purification system.

2.2. Preparation of surfactant mediated CSA doped GN/GNP@ PANI composite nanofibers

The CSA doped GN/GNP@ PANI composite nanofibers were prepared with CTAB as surfactant by the in situ chemical oxidative polymerization of aniline with GN and GNP. Ammonium persulfate (APS) was used for oxidizing purpose. GNPs were mixed with a 1 M HCl solution and ultrasonicated for even and smooth dispersion before mixing with aniline monomer. Similarly, GN was also ultrasonicated in 1 M HCl solution with CTAB. Aniline in 1 M HCl solution was then poured dropwise to the above solution, and stirred vigorously to allow proper mixing with GN and GNP, that was later polymerized by the mixing of an oxidant prepared in a 1 M HCl solution. The reaction mixture was constantly stirred for 24 h. The resulting mixture changed slowly into greenish black slurry, which was filtered and washed with double distilled water and methanol until the filtrate was colorless and it became free from all the excess acid, APS and oligomers. The HCl doped GN/GNP@ PANI composite nanofibers were de doped in a 1 M ammonia solution. Thus, the synthesized emeraldine base from of the GN/GNP@ PANI composite nanofibers was re doped with 200 mL of 0.5 M CSA. The CSA doped GN/GNP@ PANI composite nanofibers were washed thoroughly and dried at 80 °C for 18 h in an air oven, converted to a fine powder for further experimentation.

2.3. Characterization and studies

X-ray diffraction (XRD, PAN analytical, X'pert PRO-MPD) in the range, 10–90° 2θ, using Cu Kα radiation (λ=0.15405 nm) was performed to investigate the structural properties of the composite nanofibers. Raman spectroscopy (InVia Reflex UV Raman microscope, Renishaw, UK) was used to examine the interaction between GNP, CSA doped PANI and GN in the composite system. The surface morphology was examined with scanning electron microscopy (SEM, Hitachi-SU70). The optical properties were investigated by ultraviolet-visible-near infrared (UV–vis-NIR, VARIAN, Cary 5000, USA) spectrophotometry. The microstructural properties were examined by field emission transmission electron microscopy (FE-TEM, TecnaiG2 F20, FEI, USA). Thermogravimetric analysis (DTGA, SDT Q600, USA) was used by heating the samples from room temperature to 800 °C at a rate of 10 °C min^{-1} in a nitrogen environment. The cyclic voltammetry (CV) of the samples was performed using a potentiostat (VersaSTAT 3, Princeton Research, USA). The experiment was performed in 0.1 M phosphate buffer solution (pH 7; 0.1% NaCl) as the supporting electrolyte at room temperature. The projection area of the electrode was 1 cm^2. The working electrodes for the CV measurement were prepared by 50 mg of each sample mixed thoroughly by adding ethyl cellulose as a binder and α-terpineol as a solvent for the paste. The DC electrical conductivity (σ) analysis and electrical conductivity retention properties were investigated using a 4-in-line probe electrical conductivity measuring instrument with a PID controlled oven (Scientific Equipment, Roorkee, India). The DC electrical conductivity was estimated using the following equation [16].

$$\rho = \rho_0/\ln 2\ (2d/t) \tag{1}$$

$$\rho_0 = 2\pi d(V/I) \tag{2}$$

$$\sigma = 1/\rho \tag{3}$$

where ρ, σ, I, V, d, and t are the DC electrical resistivity, conductivity ($S\ cm^{-1}$), current (A), voltage (V), probe spacing (cm), and thickness of the pellet (cm), respectively.

3. Result and discussion

3.1. Morphological and structural studies

Fig. 1(a) and (b) shows SEM images of CTAB mediated CSA doped PANI and GN/GNP@ PANI composite nanofibers. The SEM images of both the CSA doped PANI and GN/GNP@ PANI revealed a uniform tubular fibrous structure. From the SEM images it is observed that the CTAB as a surfactant provided the micelle structure promoting the dense fibers for PANI and GN/GNP@ PANI (Fig. 1(a) and (b)). Fig. 1(c) and (d) show the TEM images of the CTAB mediated CSA doped GN/GNP@ PANI composite nanofibers. From the TEM images (Fig. 1(c) and (d)) it is clearly observed that GN is homogeneously and thoroughly mixed with the PANI matrix in its entirety. Fig. 1(c) clearly showed the presence of GNPs and its dispersion throughout the PANI matrix suggesting the successful incorporation of GN and GNPs into CTAB mediated CSA doped GN/GNP@ PANI composite nanofibers.

Fig. 1(e) shows the XRD pattern of the CTAB mediated CSA doped PANI and GN/GNP@ PANI composite nanofibers. The XRD pattern of CTAB mediated CSA doped PANI and GN/GNP@ PANI composite nanofibers revealed all the peaks pertaining to GNP, GN and PANI and matched well with the previous reported work. Presence of all the peaks of GNP and GN in the composite structure confirmed the success of the synthesis of the CTAB mediated CSA doped GN/GNP@ PANI composite nanofibers. The diffraction peaks at 15.5° and 25.3° corresponds to (011) and (200) planes of PANI, the peak at 25.3° can be ascribed to the periodicity perpendicular to the PANI matrix [17]. The diffraction peak at 26.5° can be related to GN in the composite structure with a d-spacing of 0.32 nm. The diffraction peaks at 38.1°, 44.4°, 64.6°, and 77.6° and 81.8° correspond to (1 1 1), (200), (2 2 0), (3 1 1) and (222) planes of GNP, respectively. Fig. 1(h) shows Raman spectra of CTAB mediated CSA doped PANI and GN/GNP@ PANI composite nanofibers. Raman spectroscopy is a well-known technique to quantify the lattice defects present in the composite system. The Raman spectra of CTAB mediated CSA doped PANI and GN/GNP@ PANI composite nanofibers were observed to be well matching with the previous reported work [18]. In the case of both the CSA doped PANI and GN/GNP@ PANI composite nanofibers, the Raman spectra bands observed at 1191, 1340, and 1592 cm^{-1} can be related to benzenoid rings, polaronic structure, and quinoid segments, respectively. Compared with CSA doped PANI the Raman spectra of CSA doped GN/GNP@ PANI showed a shift from 1592 to 1621 cm^{-1}, which might be due to the presence of GNP in the composite structure.

3.2. Thermogravimetric analysis (TGA)

Fig. 2 shows the plot of thermogravimetric analysis of CTAB mediated CSA doped PANI and GN/GNP@ PANI composite nanofibers. It can be observed that both the CSA doped PANI and GN/

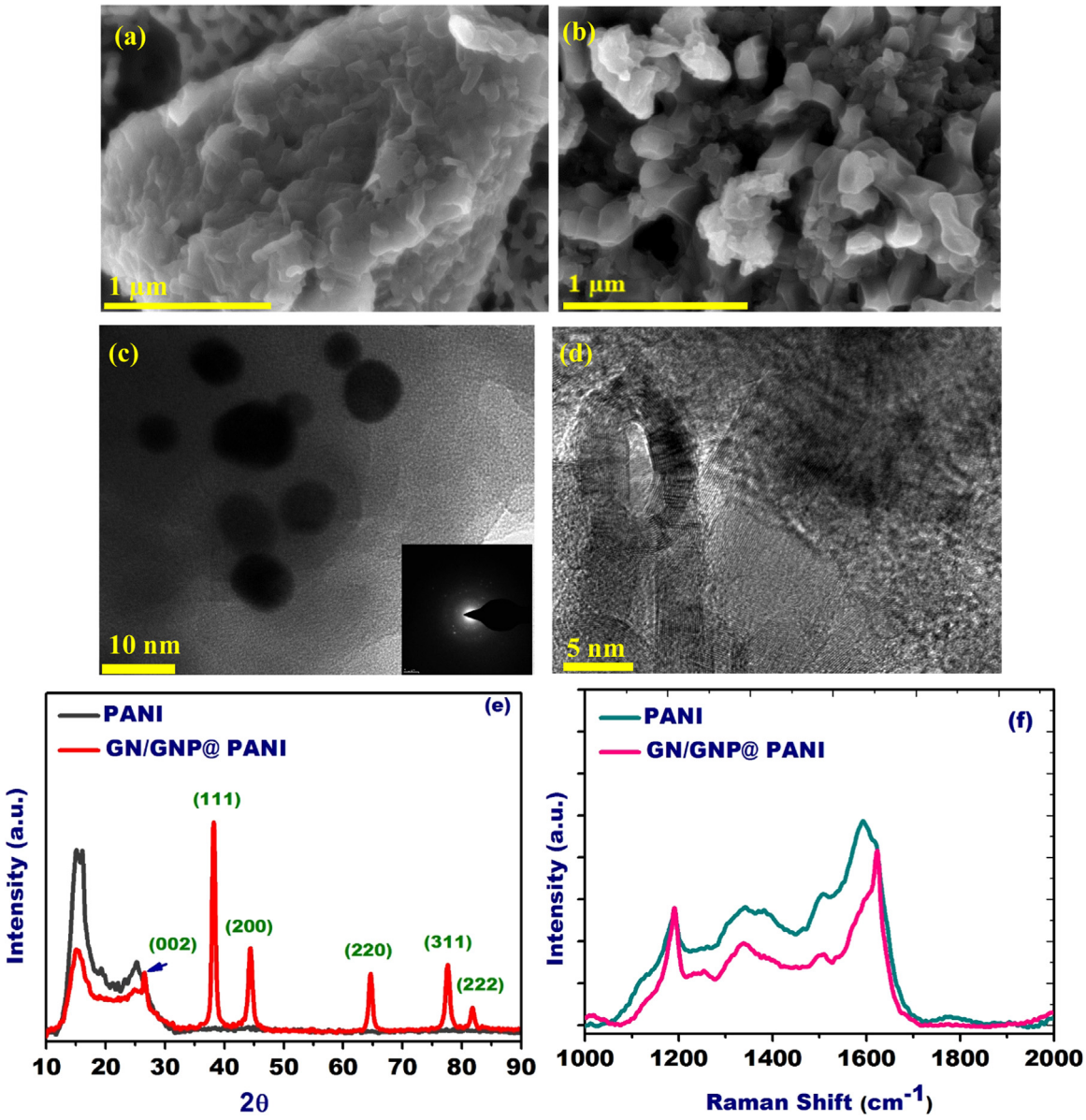

Fig. 1. SEM images of (a) CTAB mediated CSA doped PANI (b) GN/GNP@PANI composite nanofibers, (c) TEM images of CTAB mediated CSA doped GN/GNP@PANI composite nanofibers at 10 nm resolution, (d) TEM images of CTAB mediated CSA doped GN/GNP@PANI composite nanofibers at 5 nm resolution, (e) XRD patterns of the CTAB mediated CSA doped PANI and GN/GNP@PANI composite nanofibers, (f) Raman spectra for CTAB mediated CSA doped PANI and GN/GNP@PANI composite nanofibers.

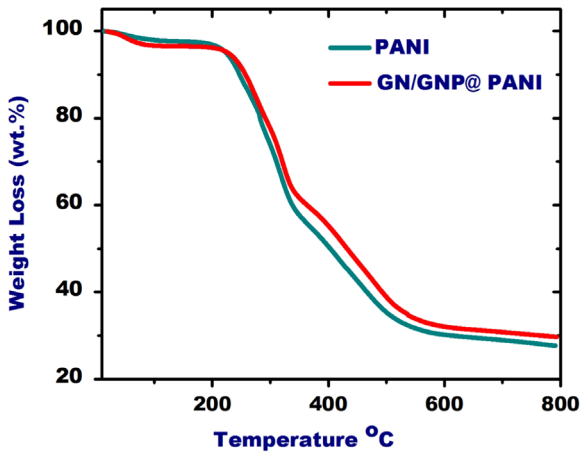

Fig. 2. TGA of the CTAB mediated CSA doped PANI and GN/GNP@PANI composite nanofibers.

GNP@ PANI composite nanofibers showed the thermal decomposition through three different weight loss stages. The first stage of weight loss was observed to be below ~200 °C which can be ascribed to the loss of moisture and the other volatile matters in the composite system. The onset temperature for the second stage of weight loss was recorded at ~240 and 250 °C for CSA doped PANI and GN/GNP@ PANI composite nanofibers, respectively. The second stage of thermal decomposition can be related to the removal of higher oligomers of PANI and surfactant CTAB. The third major weight loss initiated at ~330 and 340 °C for CSA doped PANI and GN/GNP@ PANI composite nanofibers, which might be due to the thermo-oxidative decomposition of PANI matrix into ammonia, aniline, methane and acetylene. Fig. 2 clearly showed that the thermal stability of the composite system improved after the incorporation of GN and GNP into PANI, which could be attributed to some sort of interaction between PANI and GN and GNP.

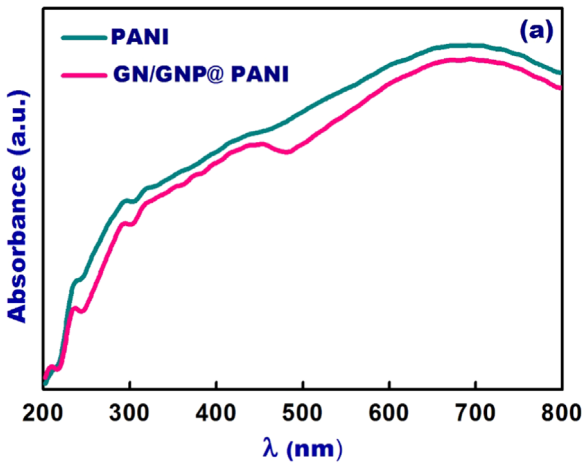

Fig. 3. (a) UV–visible diffuse absorbance spectra of CTAB mediated CSA doped PANI and GN/GNP@PANI composite nanofibers, (b) UV–visible diffuse reflectance spectra of CTAB mediated CSA doped PANI and GN/GNP@PANI composite nanofibers, (c) direct optical band gap for CTAB mediated CSA doped PANI and GN/GNP@PANI composite nanofibers.

3.3. Optical properties

Fig. 3(a) shows the UV–vis diffuse absorbance spectra of CTAB mediated CSA doped PANI and GN/GNP@ PANI composite nanofibers. Absorption peaks were revealed at ~435 and at around ~690 nm, which might be ascribed to π–π* transition of benzenoid and quinoid ring, respectively. The absorbance spectra confirmed that the synthesized GN/GNP@ PANI composites were in the doped state. From the absorbance spectra (Fig. 3(a)), It can also be seen that the GN/GNP@ PANI composite nanofibers showed similar absorption spectra with little reduced intensity compared with PANI. It can be observed that the absorption peak of the GN/GNP@ PANI composite nanofibers compared with PANI showed no shift, which inferred no change in the doped state of GN/GNP@ PANI composite nanofibers.

3.4. DC electrical conductivity and thermal stability in terms of conductivity retention

Fig. 4(a) shows the DC electrical conductivity of CTAB mediated CSA doped PANI and GN/GNP@ PANI composite nanofibers at room temperature. The room temperature DC electrical conductivity was calculated to be 4.4, 5.2 and 7 (S/cm) for CTAB mediated CSA doped PANI, PANI/GN and GN/GNP@ PANI composite nanofibers, respectively. The CTAB mediated CSA doped GN/GNP@ PANI composite nanofibers compared to PANI showed remarkable higher DC electrical conductivity at room temperature which might be due to the electronic interaction of GNP and GN with PANI. The conductivity of the nanocomposite fibers compared with PANI was increased by 59%. Fig. 4(b) shows the variation of DC electrical conductivity with temperature CTAB mediated CSA doped PANI and GN/GNP@ PANI composite nanofibers. In the case of CTAB mediated CSA doped PANI, the DC electrical conductivity increased to 6.6 (S/cm) at temperature 106 °C, after this the electrical conductivity was observed to be decreasing. However, in the case of CTAB mediated CSA doped GN/GNP@ PANI composite

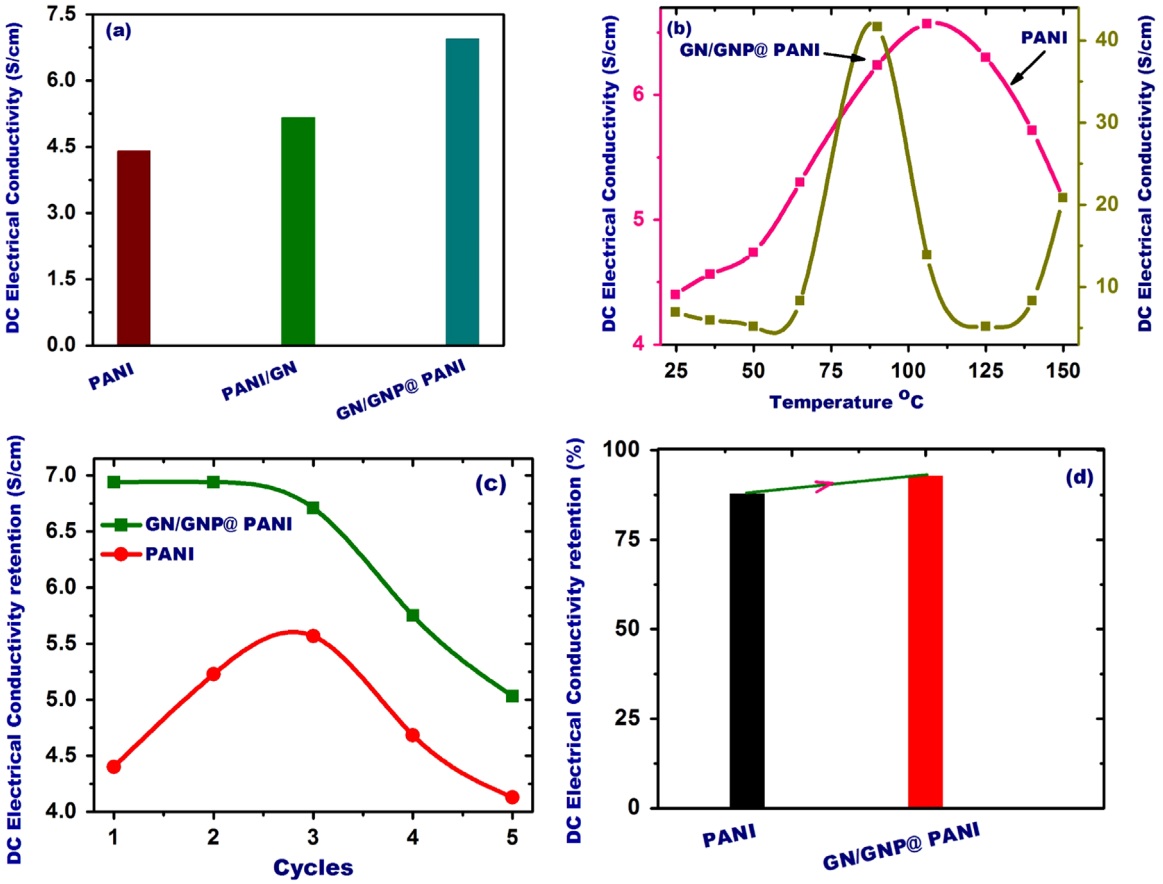

Fig. 4. (a) DC electrical conductivities of CTAB mediated CSA doped PANI, PANI/GN and GN/GNP@PANI composite nanofibers, (b) DC electrical conductivities versus temperature for CTAB mediated CSA doped PANI and GN/GNP@PANI composite nanofibers, (c) cyclic DC electrical conductivity retention at ambient temperature for CTAB mediated CSA doped PANI and GN/GNP@PANI composite nanofibers, (d) DC electrical conductivity retention percentage for CTAB mediated CSA doped PANI and GN/GNP@PANI composite nanofibers.

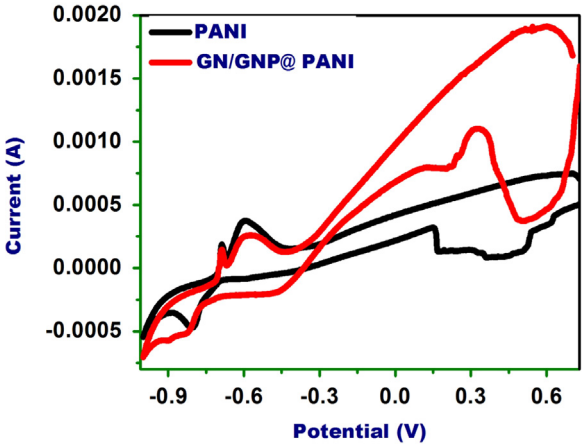

Fig. 5. Cyclic voltammetry (CV) measurement results of CTAB mediated CSA doped PANI and GN/GNP@PANI composite nanofibers.

nanofibers, the DC electrical conductivity increased to 42 (S/cm) at temperature 90 °C, after this the conductivity was shown to be decreasing (Fig. 4(b)). With increase in temperature, the decrease in DC electrical conductivity was observed for both CTAB mediated CSA doped PANI and GN/GNP@ PANI composite nanofibers respectively, which can be related to the loss of moisture. The presence of moisture increases the charge delocalization by solvating the negative anions present in the composite structure and minimizing the electrostatic interaction between the positive and negative charges [19]. Loss of moisture caused an enhancement in localization of charge and thereby reduced the DC electrical conductivity at elevated temperature [19,20]. Fig. 4(c) shows the cyclic DC electrical conductivity retention at room temperature for CTAB mediated CSA doped PANI and GN/GNP@ PANI composite nanofibers. CTAB mediated CSA doped GN/GNP@ PANI composite nanofibers showed a drop in electrical conductivity with increase in cycle. However, the CSA doped PANI showed an increase in electrical conductivity up to cycle three, then a drop. Fig. 4(d) shows the DC electrical conductivity retention for CTAB mediated CSA doped PANI and GN/GNP@ PANI composite nanofibers. In case of CTAB mediated CSA doped PANI, the retention in electrical conductivity was calculated to be 88%, while in the case of CTAB mediated CSA doped GN/GNP@ PANI composite nanofibers, the retention was observed to be 93%. DC electrical conductivity retention for both CTAB mediated CSA doped PANI and GN/GNP@ PANI composite nanofibers were obtained using the following calculation method.

$$\text{Retention}\ (\%) = \left(\sigma_{\text{cycle1, ambient temperature}} - \sigma_{\text{cycle5, 150°C}}\right) / \sigma_{\text{cycle1, ambient temperature}} \cdot 100 \quad (4)$$

The DC electrical conductivity in PANI is caused by charge transport along the conjugated chains of PANI with inter chain polaron hopping as the charge transfer mechanism. CTAB mediated CSA doped GN/GNP@ PANI composite nanofibers compared with CTAB mediated CSA doped PANI showed a remarkable enhancement in DC electrical conductivity as well as an excellent electrical conductivity retention properties. The thermal stability of the composite system was observed to be excellent as after various cycle of heat treatment, the drop in electrical conductivity was observed to be low. The enhancement in conductivity of the composite structure can be ascribed to the possible reduced hopping distance, enhanced charge carrier density and better electronic interaction between PANI and GN and GNP.

3.5. Electrochemical studies

Fig. 5 shows the cyclic voltammetry (CV) measurements for the CTAB mediated CSA doped GN/PANI and GN/GNP@PANI composite nanofibers in the voltage range from −1 to +1 V, at a scan rate of 10 mV s^{-1}. CV is known to be a powerful technique in order to determine the redox behavior and electron transfer kinetics of any system [21]. CV plays an important role in characterizing the performance of various electrical energy storage devices, such as batteries, fuel cells and electrochemical capacitors [21]. For both the CTAB mediated CSA doped GN/PANI and GN/GNP@PANI composite nanofibers, a prominent anodic and cathodic peak was revealed at −0.59 and +0.54 V, respectively. Compared with the PANI/GN the CTAB mediated CSA doped GN/GNP@PANI composite nanofibers showed greater electrochemical activity, which might be due to GN and GNP providing the larger specific are to the composite system leading to greater number of electrochemically –active sites. The enhanced capacitive performance of the CTAB mediated CSA doped GN/GNP@PANI composite nanofibers can be ascribed to homogeneous mixing of GNPs in the composite system improving the charge storage ability.

4. Conclusions

In this work, we report the synthesis of CTAB mediated CSA doped PANI and GN/GNP@ PANI composite nanofibers by in-situ oxidative chemical polymerization of aniline with GN and GNP. The detail physico-chemical characterization of nanocomposite fibers were performed using variety of techniques such as TEM, SEM, XRD, Raman spectroscopy; UV–visible diffused reflectance spectroscopy and TGA. The CTAB mediated CSA doped composite nanofibers showed higher DC electrical conductivity and conductivity retention at ambient temperature than that of PANI, which might be due to the enhancement in the mobility of the charge carriers and reduction in hopping distance and better electronic interaction between PANI, GN and GNP in the composite system. The CTAB mediated CSA doped composite nanofibers compared to PANI showed 59% and 6% higher DC electrical conductivity and conductivity retention, respectively. Moreover, the CTAB mediated CSA doped composite nanofibers showed an improvement in electrochemical activity and proved to be a better capacitor. Also the optical bandgap of the composite nanofibers was observed to be lower than that of PANI.

Acknowledgement

There is no funding source for this research.

References

[1] D.Y. Liu, J.R. Reynolds, ACS Appl. Mater. Interfaces 2 (2010) 3586.
[2] S. Palaniappan, S.L. Devi, J. Appl. Polym. Sci. 107 (2008) 1887.
[3] J. Zhao, Z. Qin, T. Li, Z. Li, Z. Zhou, M. Zhu, Prog. Nat. Sci. Mater. Int. 25 (2015) 316.
[4] A. Mostafaei, A. Zolriasatein, Prog. Nat. Sci. Mater. Int. 22 (2012) 273.
[5] M. Hasan, M. Lee, Prog. Nat. Sci. Mater. Int. 24 (2015) 579.
[6] Z.F. Liu, Q. Liu, Y. Huang, Y.F. Ma, S.G. Yin, X.Y. Zhang, Adv. Mater. 20 (2008) 3924.
[7] J.T. Robinson, F.K. Perkins, E.S. Snow, Z.Q. Wei, P.E. Sheehan, Nano Lett. 8 (2008) 3137.
[8] M. Hasan, M.M. Hossain, M. Lee, J. Ind. Eng. Chem. (2015), http://dx.doi.org/10.1016/j.jiec.2015.08.007.
[9] C. Basavaraja, W.J. Kim, Y.D. Kim, D.S. Huh, Mater. Lett. 65 (2011) 3120.
[10] S. Stankovich, D.A. Dikin, G.H.B. Dommett, K.M. Kohlhaas, E.J. Zimney, E. A. Stach, Nature 442 (2006) 282.
[11] K. Mallick, K. Mandal, M.J. Witcomb, A. Deshmukh, M. Scurrell, Mater. Sci. Eng.

B 150 (2008) 43.
[12] Q. Wu, Y. Xu, Z. Yao, A. Liu, G. Shi, ACS Nano 4 (2010) 1963.
[13] J.S. Shayeh, A. Ehsani, M.R. Ganjali, P. Norouzi, B. Jaleh, Appl. Surf. Sci. 353 (2015) 594.
[14] D. Saini, T. Basu, Appl. Nanosci. 2 (2012) 467.
[15] F. Chen, H.D. Wei, W.Y. Sheng, F. Ming, G. Xin, Z.Z. Liang, Chin. Phys. B 8 (2015) 087801.
[16] C.W. Wang, Z. Wang, M.K. Li, H.L. Li, Chem. Phys. Lett. 341 (2001) 431.
[17] W. Wu, D. Pan, Y. Li, G. Zhao, L. Ging, S. Chen, Electrochim. Acta 152 (2015) 126.
[18] D. Saini, T. Basu, Appl. Nanosci. 2 (2012) 467.
[19] V.M. Mzendaa, S.A. Goodmana, F.A. Aureta, L.C. Prinsloob, Synth. Met. 127 (2002) 279–283.
[20] J.B. Yadav, R.K. Puri, V. Puri, Appl. Surf. Sci.. 254 (2007) 1382.
[21] H. Wang, L. Pilon, Electrochim. Acta 64 (2012) 130–139.